Int J Clin Exp Pathol 2015;8(2):2221-2234
www.ijcep.com /ISSN:1936-2625/IJCEP0004055

Original Article

Ultrasound-mediated microbubble destruction enhances the therapeutic effect of intracoronary transplantation of bone marrow stem cells on myocardial infarction

Xuefeng Chang[1], Jiaqing Liu[2], Xudong Liao[3], Guohui Liu[1]

[1]*Department of Emergency Surgery, First Hospital of Jilin University, Changchun 130021, Jilin, China;*
[2]*Department of Radiation Medicine, School of Public Health of Jilin University, Changchun 130021, Jilin, China;*
[3]*Department of Cardiology, Affiliated Hospital of Beihua University, Jilin 132011, China*

Received November 22, 2014; Accepted January 28, 2015; Epub February 1, 2015; Published February 15, 2015

Abstract: Objective: The combination of intracoronary transplantation and ultrasound-mediated microbubble destruction may promote effective and accurate delivery of bone marrow stem cells (BMSCs) into the infarct zone. To test this hypothesis in this study we examined the effectiveness of ultrasound-mediated microbubble destruction in combination with intracoronary transplantation of BMSCs for the treatment of myocardial infarction in canine model of acute myocardial infarction. Method: The dogs were randomly assigned to four groups: PBS, ultrasound-mediated microbubble destruction, BMSCs, BMSCs together with ultrasound-mediated microbubble destruction. At 28 days post-surgery, cardiac function and the percentage of perfusion defect area to total left ventricular perfusion area (DA%) were determined by myocardial contrast echocardiography. Nitro blue tetrazolium staining was performed to determine myocardial infarct size, hematoxylin and eosin staining for assessing microvascular injury, Masson's staining for analyzing myocardial tissue collagen, immunohistochemical analysis of α-actin to measure cardiac contractile function and of BrdU-labeled myocardial cells to measure the number of the BMSCs homing to the infarcted region. Results: The transplantation of BMSCs significantly improved heart function and DA% ($P < 0.05$). The group that received ultrasound-mediated microbubble destruction with BMSCs transplantation showed the most improvement in heart function and DA% ($P < 0.05$). This group also showed a denser deposition of BMSCs in the coronary artery and more BrdU positive cells in the infarcted region, had the maximum number of α-actin positive cells, showed the smallest myocardial infarct area compared to other groups ($P < 0.05$). Conclusion: Ultrasound-mediated microbubble destruction increases the homing of BMSCs in the target area following intracoronary transplantation, which allows more BMSCs to differentiate into functional cardiomyocytes, thereby reducing myocardial infarct size and improving cardiac function.

Keywords: Myocardial infarction, diagnostic ultrasound-mediated microbubble destruction, bone marrow stem cells, intracoronary transplantation

Introduction

About 1.1 million new cases of acute myocardial infarction (AMI) occur yearly worldwide. AMI results in substantial myocardial necrosis, ultimately leading to ventricular remodeling and the deterioration of cardiac function. In later stages, approximately one-third of the patients with AMI suffer from heart failure or cardiogenic shock. The most commonly used treatments for AMI include drug therapy and interventional treatment, but none of these treatments increase the number of myocardial cells following myocardial infarction [1].

Animal studies and clinical investigations have suggested that bone marrow stem cells (BMSCs) effectively improve systolic function after myocardial infarction [2-4]. BMSCs also improve left ventricular remodeling in patients with acute or chronic ischemic cardiomyopathy [5-10]. BMSCs differentiate into myocardial tissue and blood vessels to reduce tissue fibrosis and release paracrine factors, ultimately reversing left ventricular remodeling [11-15]. In addition, BMSCs stimulate the proliferation of endogenous myocardial stem cells [16]. Therefore, transplantation of BMSCs offers a promising treatment for AMI. Furthermore, recent

clinical trials have shown that transplantation of allogenic BMSCs is as safe and effective as autologous BMSCs for heart tissue reconstruction [17]. The concern of immune rejection is minimal due to the lack of major histocompatibility complex class II antigen [18] and type 2 T helper cell cytokines in allogenic BMSCs [19].

The number of BMSCs homing to the infarcted region is important for determining the efficacy of stem cell transplantation. The key is to deliver sufficient stem cells safely and specifically into the infarct zone. The delivery of BMSCs can be achieved by several methods, including intracoronary transplantation, intravenous transplantation, epicardial transplantation and endomyocardial transplantation. Each method has its own advantages and disadvantages. Although epicardial and endomyocardial transplantations can ensure sufficient delivery of BMSCs into the infarcted area, it is difficult to determine the depth of puncture and accurately locate the area of myocardial infarction. These limitations can potentially lead to problems, such as cardiac rupture. Furthermore, most of BMSCs delivered by intramyocardial injection die after four days, severely limiting the clinical application [21, 22]. In contrast, BMSCs delivered by intracoronary transplantation through over-the-wire (OTW) catheter migrate and adhere to the intimal surface of the coronary arteries, and further home to the infarcted area, where they differentiate and regenerate. Therefore, accurate positioning is achieved without thoracotomy or cardiac puncture. Another major advantage of this procedure is the low risk and the ease of performing. These factors make intracoronary transplantation, in theory, the best way for transplantation of BMSCs.

The BMSCs enter the infarcted area through the gaps between the vascular endothelial cells. The absence of large enough gaps hinders complete homing of BMSCs. Ultrasound-mediated microbubble destruction could increase vascular permeability and facilitate the homing of BMSCs into myocardial infarction zone [23-25]. Ultrasound-mediated microbubble destruction also promotes the production of vascular endothelial growth factor (VEGF) and other angiogenic growth factors, which promote angiogenesis [24]. The cavitation effect also results in a local inflammatory response, which leads to the accumulation of inflammatory cytokines and endothelial cell adhesion molecules, and enhances the adhesion of transplanted BMSCs to endothelial cells by inducing changes in the myocardial microenvironment [26-28]. In addition, recent data have shown that ultrasound-mediated microbubble destruction combined with stem cell transplantation can promote MSC homing to the infarcted myocardium without producing adverse effects on the proliferation and apoptosis of the transplanted stem cells [29].

Based on the findings from previous studies, we hypothesized that the combination of intracoronary transplantation and ultrasound-mediated microbubble destruction could promote effective and accurate delivery of BMSCs into the infarct zone. To test our hypothesis, we established an AMI model in dogs and examined the efficacy of ultrasound-mediated microbubble destruction combined with intracoronary transplantation of BMSCs for the treatment of myocardial infarction.

Materials and methods

Animals

Twelve male and 12 female healthy beagle dogs (weight 15.0-18.0 kg) were obtained from the Experimental Animal Center of Jilin Provincial Academy of Traditional Chinese Medicine. Prior to initiating the experiments, the dogs were kept in cages for 2 to 3 days at 20°C with free access to food and water. The dogs were randomly divided into four groups: (i) PBS group, (ii) ultrasound microbubble + PBS group, (iii) BMSCs group, and (iv) ultrasound_microbubble + BMSCs group. Six dogs were included in each group. The operations were performed in accordance with "Guidelines for Care and Use of Experimental Animals" issued by the Ministry of Science of China in 2006.

Dogs in the ultrasound + BMSCs group underwent ultrasound-mediated microbubble destruction followed by BMSCs transplantation. While the ultrasound was performed, a micropump was used to infuse 2 mL of SonoVue at the slow rate of 1.5 mL/min. A VIVID 7D 3S ultrasound probe was used at a frequency of 1MHz and at strength of 1.0 W/cm^2. The time trigger mode was used. The trigger pulse duration was 23 ms, frame rate (FPS) was 0.5 and the trigger interval was 2 s. The mechanical

Table 1. Cardiac functions and DA% of each group (n = 6, mean ± s)

Group	EDV (ml)			LVEF (%)			FS (%)			DA (%)			D%			WMSI		
	1	2	3	1	2	3	1	2	3	1	2	3	1	2	3	1	2	3
A	27.00 ± 4.47	69.00 ± 4.65	67.00 ± 4.38#,*	77.33 ± 5.16	31.50 ± 5.16	36.50 ± 5.05#,*	48.00 ± 4.73	16.00 ± 4.73	18.50 ± 4.81#,*	0.00 ± 0.00	11.17 ± 1.48	11.19 ± 1.43#,*	38.50 ± 5.46	13.83 ± 8.28	9.83 ± 5.08#,*	1.00 ± 0.00	3.17 ± 1.17#,*	3.17 ± 1.17#,*
B	24.50 ± 4.23	70.17 ± 4.54	71.83 ± 4.49#,*	78.50 ± 5.13	35.33 ± 5.15	37.17 ± 5.04#,*	46.83 ± 4.71	16.50 ± 4.81	17.67 ± 4.80#,*	0.00 ± 0.00	11.16 ± 1.42	11.25 ± 1.88#,*	38.67 ± 5.24	8.67 ± 5.20	12.17 ± 6.37#,*	1.00 ± 0.00	3.17 ± 0.98#,*	3.17 ± 0.98#,*
C	25.50 ± 4.28	67.67 ± 4.50	37.33 ± 4.37#	75.50 ± 5.09	36.17 ± 5.15	53.17 ± 5.04#	45.83 ± 4.71	18.67 ± 4.80	28.50 ± 4.76#	0.00 ± 0.00	11.32 ± 1.59	7.11 ± 1.63#	38.83 ± 5.70	9.50 ± 5.58	21.67 ± 5.47#	1.00 ± 0.00	2.0 ± 0.00#	2.0 ± 0.00#
D	23.50 ± 4.32	66.00 ± 4.73	30.50 ± 4.23	80.17 ± 5.15	34.83 ± 5.16	65.83 ± 5.19	48.33 ± 4.71	18.00 ± 4.73	37.17 ± 4.71	0.00 ± 0.00	11.44 ± 1.33	4.56 ± 1.13	39.83 ± 5.78	8.17 ± 5.49	30.50 ± 6.19	1.00 ± 0.00	1.50 ± 0.55	1.50 ± 0.55

Note: A-D are PBS, ultrasound + PBS, BMSCs, and Ultrasound + BMSCs groups, respectively. The numbers 1-3 are respectively before AMI modeling, 4 h after AMI modeling, and 28 d after AMI modeling.

index was 1.3, total reaction time was 10 min with a depth of 8-10 cm. The ultrasound probe was fixed on the canine cardiac papillary muscle short-axis. After ultrasound-mediated microbubble destruction, 2×10^7 BrdU-labeled third generation BMSCs were delivered into the coronary artery via OTW balloon catheter. Dogs in the BMSCs group were injected with BMSCs in the same manner. Dogs in the ultrasound + PBS group received ultrasound-mediated microbubble destruction prior to receiving 2 mL intracoronary PBS injection. Dogs in the PBS group received 2 mL intracoronary PBS injection.

Reagents

DAB chromogenic enzyme substrate kit was purchased from Boster (Wuhan, China). Mouse monoclonal anti-BrdU antibody was from SANTA, USA. L-DMEM medium was from Invitrogen (Carlsbad, CA, USA) and Percoll stock solution from Sigma (St. Louis, MO, USA). CD34 and CD44 rabbit monoclonal antibodies were from Dingguo Biotechnology (Beijing, China). The 2.5 mm × 15 mm OTW balloons were from Medtronic (Minneapolis, MN, USA).

BMSCs preparation

The healthy dogs were anesthetized 3 h weeks before transplantation by intraperitoneal injection of 5% pentobarbital (1 mL/kg). After iodine disinfection, bone marrow aspirate (10 mL) was drawn from canine humerus with a syringe needle and mixed with an equal volume of heparin. BMSCs were purified by Percoll density gradient centrifugation and seeded in a 100 mm culture dish in L-DMEM medium supplemented with fetal calf serum (FSC), 100 U/mL penicillin, and 0.1 mg/mL streptomycin at 37°C with 5% CO_2. After 24 h the medium was changed to remove non-adherent cells, such as red blood cells and macrophages. BMSCs were passaged at 70% confluency. The cells were passaged in a 1:3 ratio, and medium was changed every two days. All assays were performed with the third generation of cells.

MTT colorimetric assay was performed to monitor the survival and growth of BMSCs. Briefly, 20 μL MTT (5 mg/mL) was added to the wells. After 4 h incubation at 37°C, the supernatant was aspirated and 150 μL dimethyl sulfoxide (DMSO) was added. After gently agitating for 10 min, absorbance (A) was measured at 490 nm using a microplate reader (Shanghai Peiou Analyticals). MTT values were measured for nine consecutive days and growth curves were plotted.

The purity of BMSCs in each generation was determined by immunohistochemical staining for CD34 and CD44 positive cells. 24 h prior to transplantation, 10 μL BrdU labeling fluid (50 mg BrdU in 0.8 mL DMSO and 1.2 mL water) was added to label BMSCs

Canine AMI modeling

The dogs were allowed to fast for 8 h, and then injected with 0.05 mg/kg atropine 15 min prior to surgery. Subsequently, the dogs were anesthetized by intraperitoneal injection of 3% sodium pentobarbital (40 mg). The dogs maintained normal temperature and spontaneous breathing in the supine position. ECG was monitored with body surface electrodes throughout the surgery. After the application of lidocaine, a local anesthesia, Seldinger right femoral artery puncture was performed and a 6F sheath was placed. 2,500 U of heparin was infused through the femoral artery at the beginning, and an additional 1,250 U heparin was infused every hour. A 6F catheter was inserted from the right femoral artery to the aortic root that was selected for angiography. A small amount of contrast agent (Iopromide 370) was injected to confirm the position of the catheter and the opening of the left coronary artery. The catheter was turned around for entry into the left main coronary artery and to view the left anterior descending artery (LAD) and the left circumflex artery. At this point, the catheter tip was moved forward slightly into LAD and further into the distal anterior descending artery with BMW guide wire. The 6F OTW balloon catheter was pushed into the interval between the first and second septal branch at a distance of 0.5-1.0 cm from the bifurcation between the LAD and the left circumflex artery. The contrast agent was infused, and the dogs received ischemic preconditioning 3-5 times at an interval of 3-5 min, with each balloon inflation lasting 20 s. The contrast agent was infused again and the OTW balloon was filled to occlude the anterior descending coronary artery. The surgery was concluded by withdrawing the balloon from the anterior descending artery after 4 h. The OTW balloon catheters, guide wires, catheters, and sheaths were removed sequentially, and the site of surgery was covered with an elastic ban-

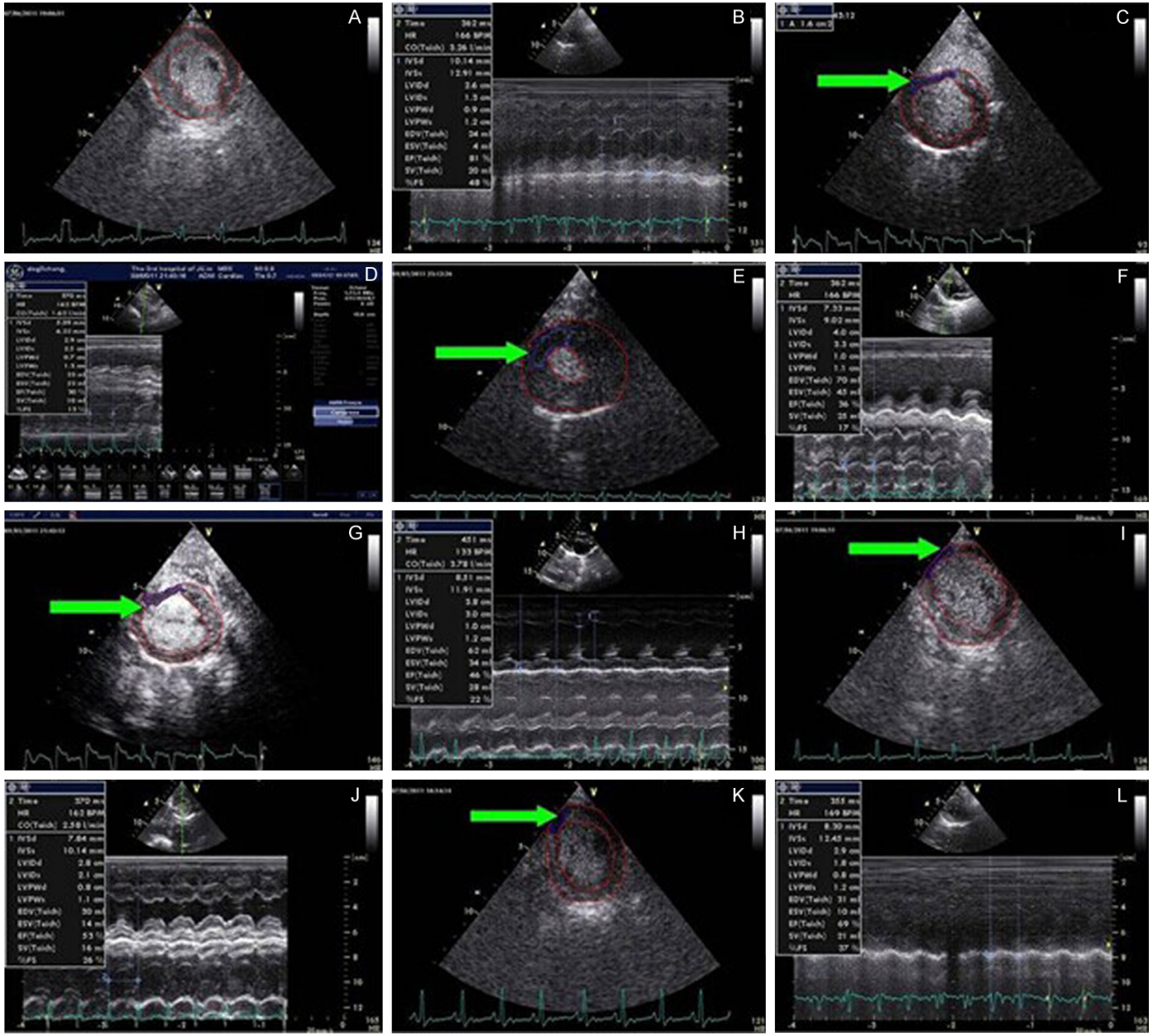
A
B
C
D
E
F
G
H
I
J
K
L

Figure 1. A: DA% before AMI modeling; B: Cardiac functions before AMI modeling; C: DA% 4 h after AMI modeling; D: Cardiac functions 4 h after AMI modeling; E: DA% of the PBS group; F: Cardiac functions of the PBS group; G: DA% of the ultrasound + PBS group; H: Cardiac functions of the ultrasound + PBS group; I: DA% of the BMSC group; J: Cardiac functions of the BMSC group; K: DA% of the ultrasound + BMSC group; L: Cardiac functions of the ultrasound + BMSC group.

Table 2. Myocardial infarct size for each group after treatment (n = 6, mean ± s)

Group	Myocardial infarct area in the cross-sectional area of left ventricle, %
PBS	11.18 ± 1.43
Ultrasound + PBS	11.24 ± 1.87
BMSCs	7.11 ± 1.60
Ultrasound + BMSCs	4.56 ± 1.09*

Note: *$P < 0.05$, Ultrasound + BMSCs group compared to all other groups.

dage for 18 h. After the surgery, the dogs were moved to clean cages with restricted activity. Dogs were given intramuscular injection of 3.0 g sodium ampicillin. The dogs that exhibited ventricular arrhythmias were intravenously injected with lidocaine (5-10 mg/kg). The dogs that experienced lowering of the heart rate were given 1 mg of epinephrine. The coronary artery stenosis or interruption of blood flow detected by coronary angiography was likely to be due to thrombosis, which was subsequently cleared by catheters to mimic the clinical process of ischemia- reperfusion.

Measurements

Coronary angiography was performed to examine whether blood flow was blocked after AMI modeling. M-mode ultrasound was used to measure cardiac function, including end-diastolic volume (EDV) (mL), end-systolic volume (ESV) (mL), left ventricular ejection fraction (LVEF) (%), fractional shortening (FS) (%), wall thickening (D%), and wall motion score index (WMSI). Left ventricular wall thickening was measured with the use of anatomical M-curve and GE VIVID 7D ultrasonic diagnostic equipment. D% = (systolic ventricular wall thickness - end-diastolic wall thickness)/end-diastolic wall thickness × 100%. LVEF was calculated by measuring EDV and ESV. WMSI was measured by visual, semi-quantitative method and two-dimensional echocardiography analysis according to the 16-segment model recommended by the American Society of Echocardiography.

DA% was measured by myocardial contrast echocardiography (MCE) using VIVID 7D ultrasonic diagnostic equipment. The 3S probe was placed on the 4^{th}-6^{th} intercostal space. Sections were referenced against left ventricular papillary muscle short-axis. Contrast program was used for intermittent harmonic imaging. 2 mL SonoVue was slowly infused through the femoral vein at 1.5 mL/min with a micropump, and was followed by a 5 mLsaline flush. After destabilization, scintigraphy was triggered to launch several high-energy pulses, which could instantly destroy the microbubble contrast agent completely within the cardiac muscles. 3-5 cardiac cycles were recorded after the contrast agent in the left ventricular cavity was at full imaging capacity. It was transitioned to low mechanical index to facilitate observation of the re-filling process. The Matlab program was modified to calculate the percentage of perfusion defect area (DA) to the total left ventricular perfusion area (DA%). Two-dimensional echocardiography was recorded each time before the completion of real-time myocardial contrast.

For the assessment of cardiac function, DA%, EDV, ESV, LVEF, FS%, D%, WMSI, simultaneous ECG lead V1 were measured at 4 h following the surgery, 7 days following the surgery, and 28 days after treatment.

Pathological and immunohistochemical analysis

28 days following treatments, dogs were sacrificed by intramyocardial injection of potassium chloride. The hearts were removed to find the blocking points in coronary LAD. Continuous cardiac cross-sections were prepared below the level of the blocking points for pathological and immunohistochemical analysis.

For the pathological analysis, conventional HE staining, Masson staining, and NBT staining were performed. On the basis of NBT staining, DA% was defined as myocardial infarct size/left ventracular cross-sectional area × 100%. Immunohistochemical analysis included α-actin and BrdU staining.

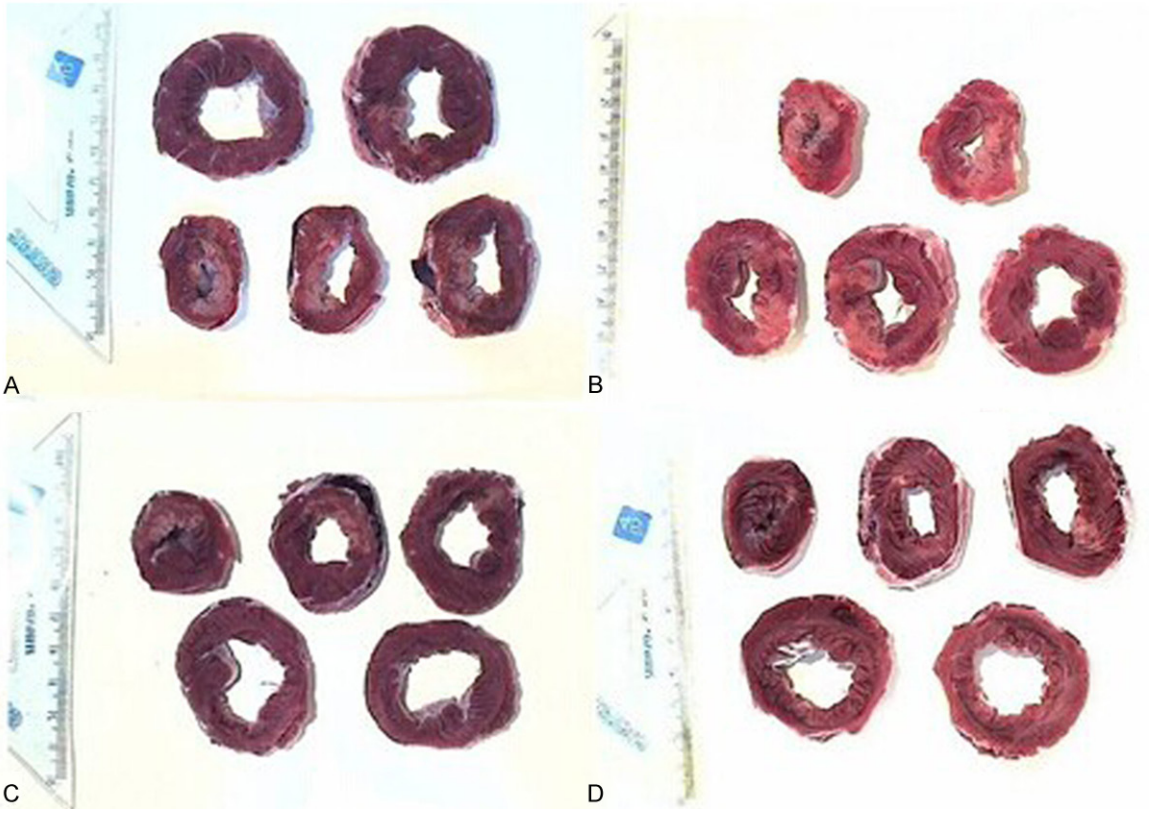

Figure 2. Heart cross-sections of (A) PBS group; (B) Ultrasound + PBS group; (C) BMSC group; (D) Ultrasound+BMSC group. Each panel shows 5 heart cross-sections of one dog in each group which correspond to the levels of the papillary muscles taken by MCE. Infarct size was calculated as the percentage of area to the left ventricular cross-section. Scale bars were shown on the left.

Statistical analysis

SPSS18.0 (PASW) and Microsoft Excel software were used for data analysis. The parameters in each experimental group at each time point were expressed as mean ± standard deviation ($\bar{x}$ ± s). The *t* test was used for comparison between two groups. Analysis of variance was used for comparison among multiple groups. $P < 0.05$ was considered significant.

Results

Evaluation of canine AMI

Smaller animals, such as the rabbit and rat, are inappropriate for AMI modeling due to the small size of their heart and coronary vessels. Therefore, in this study, we used the dog as the experimental model of AMI.

The measurements of cardiac ultrasound, MCE functions and DA% 4 h, 7 days and 28 days following surgery were shown in **Table 1** and **Figure 1A-D**. The results showed that within each group, cardiac functions were significantly decreased while DA% was significantly increased ($P < 0.05$) at 4 h post-surgery. Coronary angiography showed that the left anterior descending artery was blocked. MCE-synchronized ECG lead V1 showed characteristic AMI changes including significantly elevated ST segment, upward arch, connecting with upright T wave to form a single curve and the pathological Q wave. These data indicate that the AMI induction was successful in all groups.

Ultrasound-mediated microbubble destruction combined with BMSCS intracoronary transplantation significantly improved AMI

The cardiac functions and DA% were measured by cardiac ultrasound and MCE 28 days after BMSCs transplantation (**Table 1**; **Figure 1E-L**). The results indicated that both ultrasound + BMSCs group and BMSCs group had significantly improved heart function and DA% ($P < 0.05$) following the delivery of BMSCs. In contrast, PBS and ultrasound + PBS groups sho-

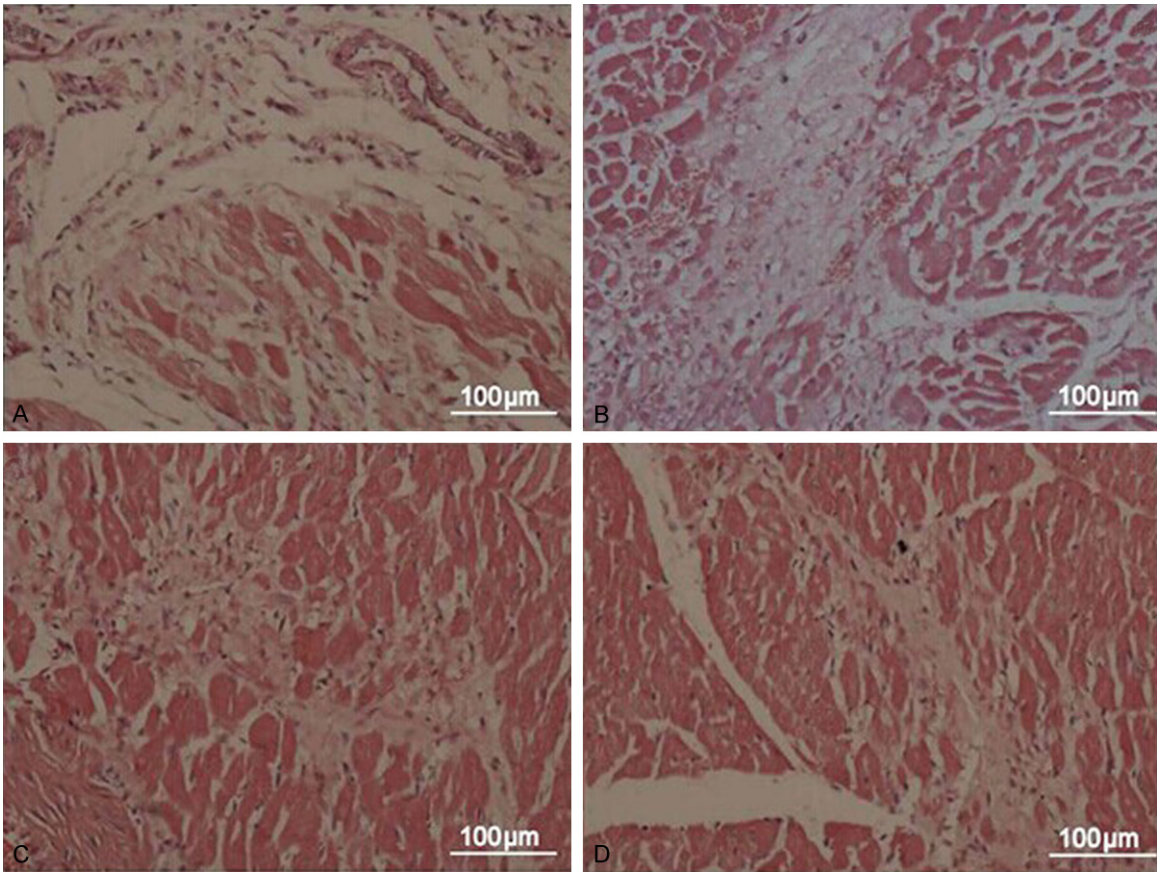

Figure 3. HE staining of heart tissues in each group. A: PBS group; B: Ultrasound + PBS group; C: BMSC group; D: Ultrasound + BMSC group.

wed no improvement in cardiac function and DA% after PBS treatment ($P > 0.05$). Compared to BMSCs, ultrasound + PBS and PBS groups, DA% in ultrasound + BMSCs group was reduced by 35.9%, 59.5%, and 59.2%, respectively, suggesting that ultrasound + BMSCs group experienced most significant improvement.

Pathological examination confirmed the results of cardiac ultrasound and MCE. Compared to BMSCs, ultrasound + PBS and PBS groups, the infarct size of ultrasound + BMSCs group was reduced by 35.9%, 59.5%, and 59.2%, respectively ($P < 0.05$). Compared to ultrasound + PBS and PBS groups, the infarct size of BMSCs group was reduced by 36.7% and 36.4%, respectively ($P < 0.05$). However, the difference in infarct size between ultrasound + PBS and PBS groups was not significant ($P > 0.05$) (**Table 2**; **Figure 2**).

According to the HE staining results, the PBS group and ultrasound + PBS group had massive fibrous scar formation in the myocardial infarction. We observed the infiltration of a small number of inflammatory cells and the formation of a few capillaries in the infarct, but found no capillaries in the fibrous scars. In contrast, in BMSCs and ultrasound + BMSCs groups, dilated capillaries filled with red blood cells formed in the fibrous scar. The myocardial infarction area was reduced in BMSCs and ultrasound + BMSCs groups compared to PBS and ultrasound + PBS groups. The maximum reduction in myocardial infarction area was observed in ultrasound + BMSCs group (**Figure 3**). In addition, Masson's staining revealed the least amount of myocardial tissue collagen in ultrasound + BMSCs group (**Figure 4**).

Ultrasound-mediated microbubble destruction promotes homing of BMSCs to myocardial infarct zone

BrdU staining showed that on the 28th day following BMSCs transplantation, the number of BrdU positive cells was significantly higher in

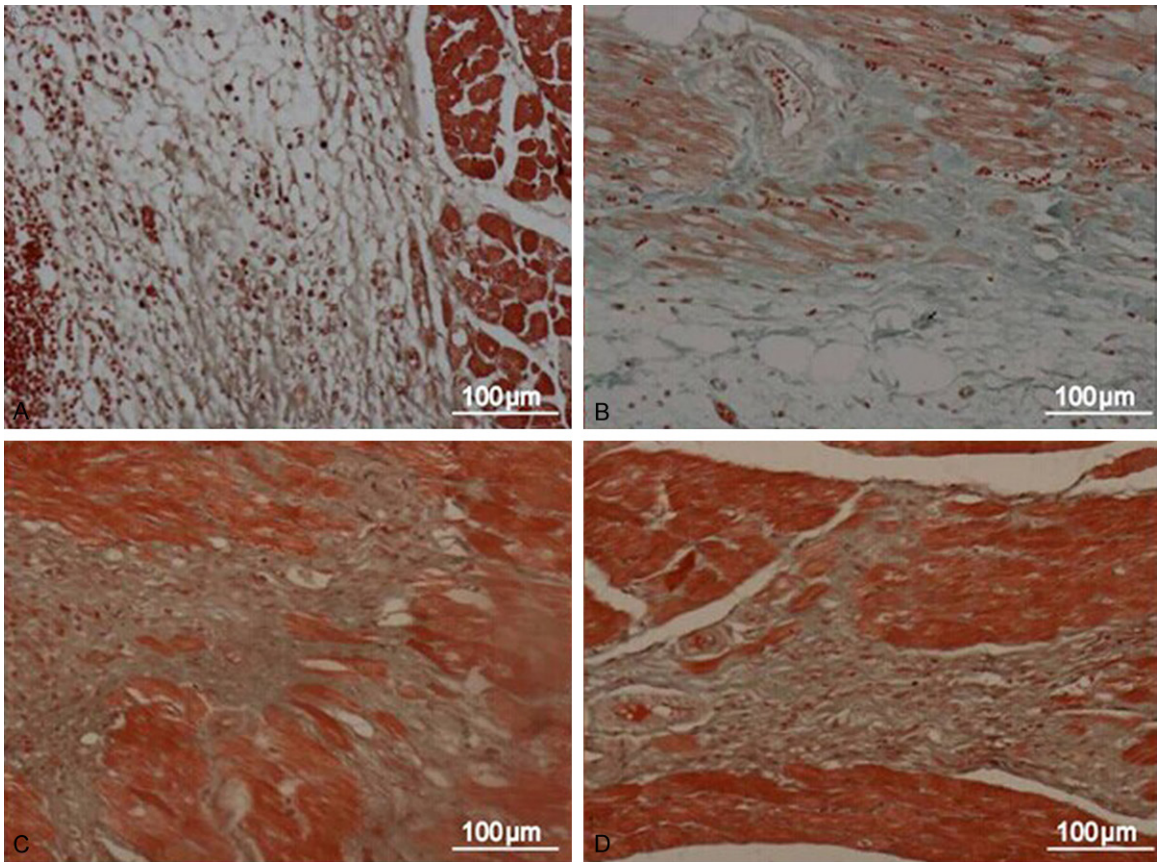

Figure 4. Masson's staining of heart tissues in each group. A: PBS group; B: Ultrasound + PBS group; C: BMSC group; D: Ultrasound + BMSC group.

the ultrasound + BMSCs group than in the BMSCs group ($P < 0.05$; **Figure 5**).

Immunohistochemical staining showed that the highest numbers of α-actin positive cells were present in the ultrasound + BMSCs group followed by the BMSCs group. In contrast, very few α-actin positive cells were observed in the myocardial infarction area of the ultrasound + PBS and PBS groups (**Figure 6**). These results suggest that ultrasound-mediated microbubble destruction promotes homing of BMSCs to myocardial infarct zone and cardiac recovery.

Discussion

In this study, we aimed to examine the efficacy of ultrasound-mediated microbubble destruction combined with intracoronary transplantation of BMSCs for the treatment of myocardial infarction in a canine model of acute myocardial infarction. Coronary angiography, pathological analysis of the infarct region and ultrasonic detection were used to assess cardiac function before and after modeling. The results suggested that transplantation of BMSCs reduced myocardial infarct size and perfusion defect area and improved heart function. More importantly, ultrasound-mediated microbubble de-struction enhanced the therapeutic effect of BMSCs by promoting the survival of cardiac muscles. This study provides pre-clinical evidence for the use of stem cells for the treatment of myocardial infarction.

Following myocardial infarction, myocardial inflammation and fibrosis occur, both of which are known to affect the survival and differentiation of transplanted BMSCs. Therefore, choosing the right time for transplantation is critical. Local lesion microenvironment is the most critical factor for the Cell survival, and it will affect the adhesion, migration and colonization capabilities and long-term survival of the transplanted cells [30]. It has been shown that stem cells die if transplanted immediately after acute myocardial infarction, as a result of the strong inflammatory response that is mounted by the host following infarction [31]. During the acute phase, which usually occurs within 48 h of myocardial infarction, interleukin-8 (IL-8) attracts

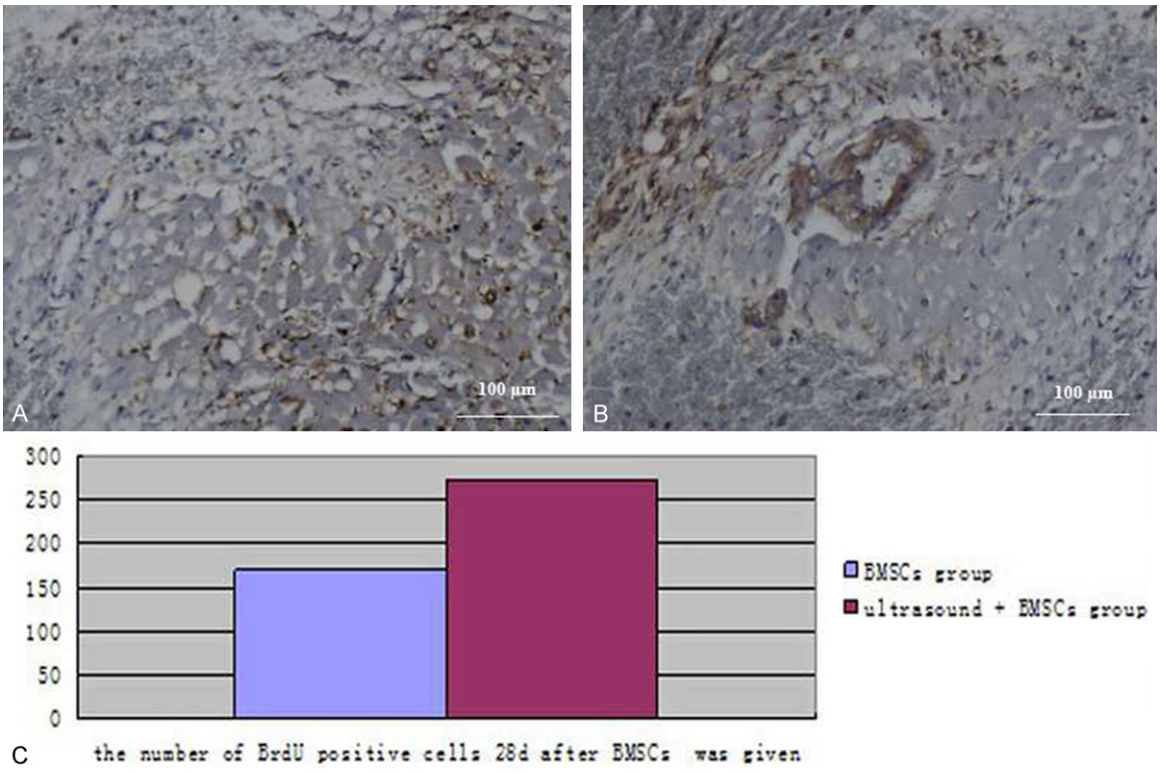

Figure 5. BrdU staining after BMSC transplantation. A: BMSC group; B: Ultrasound + BMSC group (× 100); C: Statistical analysis of BrdU positive cells.

neutrophils to the myocardial infarct. The neutrophils release proteolytic enzymes that attack transplanted BMSCs. The necrotic BMSCs are eventually cleared by the macrophages. Previous studies have recommended transplanting BMSCs 2-5 days after AMI to achieve the best therapeutic effect [18]. The homing of stem cells to the ischemic area in the heart depends on the adhesion of homing factors to endothelial cells [32]. The factors involved in the homing process are either weakened or completely disappear after a significant duration of time [33]. Therefore, it is critical to choose an appropriate time for stem cell transplantation. It has been reported that VEGF secretion peaks at day 7 after myocardial infarction [34]. In addition, from day 7 to day 15, inflammation decreases while the formation of fibrous tissue is not complete. This period of time is most conducive for BMSCs survival. Therefore, we chose to transplant BMSCs 7 days after AMI modeling. Our results confirmed that BMSCs survived and differentiated following transplantation.

Previous studies have shown that in rabbits, intravenous transplantation combined with diagnostic ultrasound microbubble destruction enhanced the homing of BMSCs to the ischemic myocardium and improved cardiac function [36-38]. However, to our knowledge, this is the first study to combine BMSCs intracoronary transplantation with diagnostic ultrasound microbubble destruction. We proposed several mechanisms to account for the efficacy of ultrasound-mediated microbubble destruction combined with BMSCs intracoronary transplantation. BMSCs differentiate into myocardial tissue and blood vessels, reduce tissue fibrosis, and release paracrine factors, ultimately reversing left ventricular remodeling [11-15]. In addition, BMSCs differentiate directly into myocardial cells, and stimulate the proliferation of endogenous myocardial stem cells [12]. Im-portantly, ultrasound-mediated microbubble destruction improves the efficacy of BMSCs treatment in several ways. It increases the permeability of neighboring endothelial cell membranes to extracellular macromolecules, widens the gaps between vascular endothelial cells and promotes the migration of transplanted BMSCs to the ischemic region [35]. Moreover, the cavitation effect generated by ultrasound-mediated microbubble destruction induces a local inflammatory response and enhances the adhesion of transplanted BMSCs to

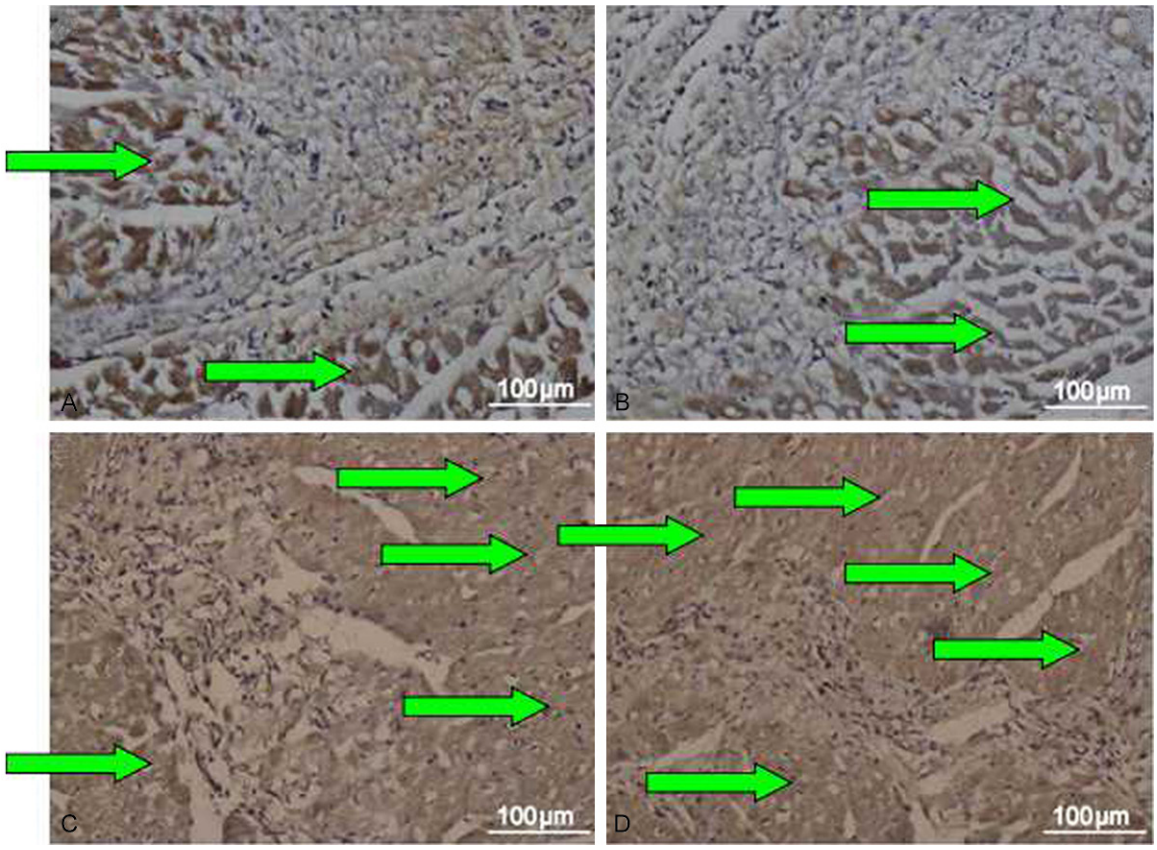

Figure 6. α-actin staining of heart tissues in each group. A: PBS group; B: Ultrasound + PBS group; C: BMSC group; D: Ultrasound + BMSC group (× 100).

endothelial cells [26-28]. It also stimulates the production of vascular endothelial growth factor (VEGF) and other angiogenic growth factors to promote angiogenesis while improving the efficacy of stem cell transplantation [24, 28]. In this study we employed intracoronary transplantation to ensure safe and accurate delivery of BMSCs into the infarcted coronary artery, thereby augmenting the benefits for BMSCs survival and proliferation that are provided by ultrasound-mediated microbubble destruction.

Positron emission tomography (PET) and pathological analysis are the gold standards for determining cardiac muscle survival following AMI. However, the high cost of PET constrains its use in both animal experiments and clinical trials. In contrast, the cost of pathological analysis is relatively low. In this study, we performed pathological analysis of myocardial infarction to confirm the success of AMI modeling and evaluate the efficacy of the treatments. NBT staining was used to evaluate myocardial infarct size, HE staining revealed the morphology of the lesions, and Masson's staining was used to observe tissue collagen. The pathological examination indicated that cardiac function improved as a result of myocardium survival and fibrosis reduction. The immunohistochemical analysis suggested that transplanted stem cells differentiated into functional cardiomyocytes. Significant improvement in cardiac function was achieved when a large number of BMSCs reached the infarct region. We also demonstrated that MCE may be used to assess myocardial viability. These results are consistent with previous findings that MCE and PET analysis show good correlation [39]. Therefore, MCE can be used as a simple and inexpensive method to evaluate myocardial cell activity in vivo.

In this study, we examined the efficacy of different treatments for myocardial ischemia or infarction via echocardiography, myocardial contrast echocardiography, coronary angiography and pathological analysis. The results obt-

ained with the different analysis were consistent. Notably, we still observed BrdU labeled BMSCs on the 28th day following BMSCs transplantation. In theory, BrdU could be stable and passed on through the process of cell division. Therefore, our finding of BrdU labeled BMSCs is not entirely unexpected.

Conclusion

Our study provides experimental evidence that ultrasound-mediated microbubble destruction can increase the homing and accumulation of BMSCs in the target area after intracoronary transplantation. Therefore, more BMSCs can differentiate into functional cardiomyocytes, reduce myocardial infarct size, and improve cardiac function. The combination of ultrasound-mediated microbubble destruction and BMSCs intracoronary transplantation represents a promising treatment for myocardial infarction.

Acknowledgements

We thank Professor Bo Sun (Jilin University School of Pharmacy) for his support, guidance and help with the experiments.

Disclosure of conflict of interest

None.

Address correspondence to: Dr. Guohui Liu, Department of Emergency Surgery, First Hospital of Jilin University, Changchun 130021, Jilin, China. Tel: 86-13331767332; E-mail: zhangxx063@sina.com

References

[1] Sanz-Rosa D, García-Prieto J and Ibanez B. The future: therapy of myocardial protection. Ann N Y Acad Sci 2012; 1254: 90-98.

[2] Tang J, Xie Q, Pan G, Wang J and Wang M. Mesenchymal stem cells participate in angiogenesis and improve heart function in rat model of myocardial ischemia with reperfusion. Eur J Cardiothorac Surg 2006; 30: 353-361.

[3] Buziashvili IuI, Matskeplishvili ST, Alekian BG, Aripov MA, Kamardinov DKh, Bokeriia LA. Acute coronary syndrome and cell technologies. Vestn Ross Akad Med Nauk 2005; 4: 65-70.

[4] Saito T, Kuang JQ, Bittira B, Al-Khaldi A and Chiu RC. Xenotransplant cardiac chimera: immune tolerance of adult stem cells. Ann Thorac Surg 2002; 74: 19-24.

[5] Leistner DM, Fischer-Rasokat U, Honold J, Seeger FH, Schächinger V, Lehmann R, Martin H, Burck I, Urbich C, Dimmeler S, Zeiher AM and Assmus B. Transplantation of progenitor cells and regeneration enhancement in acute myocardial infarction (TOPCARE-AMI): final 5-year results suggest long-term safety and efficacy. Clin Res Cardiol 2011; 100: 925-934.

[6] Schächinger V, Assmus B, Erbs S, Elsässer A, Haberbosch W, Hambrecht R, Yu J, Corti R, Mathey DG, Hamm CW, Tonn T, Dimmeler S, Zeiher AM and REPAIR-AMI investigators. Intracoronary bone marrow-derived progenitor cells in acute myocardial infarction. N Engl J Med 2006; 355: 1210-1221.

[7] Hare JM, Traverse JH, Henry TD, Dib N, Strumpf RK, Schulman SP, Gerstenblith G, DeMaria AN, Denktas AE, Gammon RS, Hermiller JB Jr, Reisman MA, Schaer GL and Sherman W. A randomized, double-blind, placebo-controlled, dose-escalation study of intravenous adult human mesenchymal stem cells (prochymal) after acute myocardial infarction. J Am Coll Cardiol 2009; 54: 2277-2286.

[8] Perin EC, Willerson JT, Pepine CJ, Henry TD, Ellis SG, Zhao DX, Silva GV, Lai D, Thomas JD, Kronenberg MW, Martin AD, Anderson RD, Traverse JH, Penn MS, Anwaruddin S, Hatzopoulos AK, Gee AP, Taylor DA, Cogle CR, Smith D, Westbrook L, Chen J, Handberg E, Olson RE, Geither C, Bowman S, Francescon J, Baraniuk S, Piller LB, Simpson LM, Loghin C, Aguilar D, Richman S, Zierold C, Bettencourt J, Sayre SL, Vojvodic RW, Skarlatos SI, Gordon DJ, Ebert RF,Kwak M, Moyé LA, Simari RD; Cardiovascular Cell Therapy Research Network (CCTRN). Effect of transendocardial delivery of autologous bone marrow mononuclear cells on functional capacity, left ventricular function, and perfusion in chronic heart failure: the FOCUS-CCTRN trial. JAMA 2012; 25: 307: 1717-1726.

[9] Assmus B, Honold J, Schächinger V, Britten MB, Fischer-Rasokat U, Lehmann R, Teupe C, Pistorius K, Martin H, Abolmaali ND, Tonn T, Dimmeler S and Zeiher AM. Transcoronary transplantation of progenitor cells after myocardial infarction. N Engl J Med 2006; 355: 1222-1232.

[10] Losordo DW, Henry TD, Davidson C, Sup Lee J, Costa MA, Bass T, Mendelsohn F, Fortuin FD, Pepine CJ, Traverse JH, Amrani D, Ewenstein BM, Riedel N, Story K, Barker K, Povsic TJ, Harrington RA, Schatz RA; ACT34-CMI Investigators. Intramyocardial, autologous CD34 + cell therapy for refractory angina. Circ Res 2011; 109: 428-436.

[11] Williams AR and Hare JM. Mesenchymal stem cells: biology, pathophysiology, translational

findings, and therapeutic implications for cardiac disease. Circ Res 2011; 109: 923-940.
[12] Karantalis V, Balkan W, Schulman IH, Hatzistergos KE and Hare JM. Cell-based therapy for prevention and reversal of myocardial remodeling. Am J Physiol Heart Circ Physiol 2012; 303: H256-H270.
[13] Quevedo HC, Hatzistergos KE, Oskouei BN, Feigenbaum GS, Rodriguez JE, Valdes D, Pattany PM, Zambrano JP, Hu Q, McNiece I, Heldman AW and Hare JM. Allogeneic mesenchymal stem cells restore cardiac function in chronic ischemic cardiomyopathy via trilineage differentiating capacity. Proc Natl Acad Sci U S A 2009; 106: 14022-14027.
[14] Schuleri KH, Amado LC, Boyle AJ, Centola M, Saliaris AP, Gutman MR, Hatzistergos KE, Oskouei BN, Zimmet JM, Young RG, Heldman AW, Lardo AC and Hare JM. Early improvement in cardiac tissue perfusion due to mesenchymal stem cells. Am J Physiol Heart Circ Physiol 2008; 294: H2002-H2011.
[15] Kudo M, Wang Y, Wani MA, Xu M, Ayub A and Ashraf M. Implantation of bone marrow stem cells reduces the infarction and fibrosis in ischemic mouse heart. J Mol Cell Cardiol 2003; 35: 1113-1119.
[16] Hatzistergos KE, Quevedo H, Oskouei BN, Hu Q, Feigenbaum GS, Margitich IS, Mazhari R, Boyle AJ, Zambrano JP, Rodriguez JE, Dulce R, Pattany PM, Valdes D, Revilla C, Heldman AW, McNiece I and Hare JM. Bone marrow mesenchymal stem cells stimulate cardiac stem cell proliferation and differentiation. Circ Res 2010; 107: 913-922.
[17] Hare JM, FFishman JE, Gerstenblith G, DiFede Velazquez DL, Zambrano JP, Suncion VY, Tracy M, Ghersin E, Johnston PV, Brinker JA, Breton E, Davis-Sproul J, Schulman IH, Byrnes J, Mendizabal AM, Lowery MH, Rouy D, Altman P, Wong Po Foo C, Ruiz P, Amador A, Da Silva J, McNiece IK, Heldman AW, George R and Lardo A. Comparison of allogeneic vs. autologous bone marrow-derived mesenchymal stem cells delivered by transendocardial injection in patients with ischemic cardiomyopathy. JAMA 2012; 308: 2369-2379.
[18] Le Blanc K, Tammik C, Rosendahl K, Zetterberg E and Ringdén O. HLA expression and immunologic properties of differentiated and undifferentiated mesenchymal stem cells. Exp Hematol 2003; 31: 890-896.
[19] Batten P, Sarathchandra P, Antoniw JW, Tay SS, Lowdell MW, Taylor PM and Yacoub MH. Human mesenchymal stem cells induce T cell anergy and downregulate T cell allo-responses via the TH2 pathway: relevance to tissue engineering human heart valves. Tissue Eng 2006; 12: 2263-2273.
[20] Strauer BE, Brehm M, Zeus T, Köstering M, Hernandez A, Sorg RV, Kögler G and Wernet P. Repair of infarcted myocardium by autologous intracoronary mononuclear bone marrow cell transplantation in humans. Circulation 2002; 106: 1913-1918.
[21] Toma C, Pittenger MF, Cahill KS, Byrne BJ and Kessler PD. Humanmesenchymal stem cells differentiate to a cardiomyocyte phenotype in the adult murine heart. Circulation 2005; 105: 93-98.
[22] Sheng CC, Zhou L and Hao J. Current stem cell delivery methods for myocardial repair. Biomed Res Int 2013; 2013: 547902.
[23] Vulliet PR, Greeley M, Halloran SM, MacDonald KA and Kittleson MD. Intra-coronary arterial injection of mesenchymal stromal cells and microinfarction in dogs. Lancet 2004; 363: 783-784.
[24] Yoshida J, Ohmori K, Takeuchi H, Shinomiya K, Namba T, Kondo I, Kiyomoto H and Kohno M. Treatment of ischemic limbs based on local recruitment of vascular endothelial growth factor-producing inflammatory cells with ultrasonic microbubble destruction. Coll Cardiol 2005; 46: 899-905.
[25] Imada T, Tatsumi T, Mori Y, Nishiue T, Yoshida M, Masaki H, Okigaki M, Kojima H, Nozawa Y, Nishiwaki Y, Nitta N, Iwasaka T and Matsubara H. Targeted delivery of bone marrow mononuclear cells by ultrasound destruction of microbubbles induces both angiogenesis and arteriogenesis response. Arterioscler Thromb Vasc Biol 2005; 25: 2128-2134.
[26] Zen K, Okigaki M, Hosokawa Y, Adachi Y, Nozawa Y, Takamiya M, Tatsumi T, Urao N, Tateishi K, Takahashi T and Matsubara H. Myocardium-targeted delivery of endothelial progenitor cells by ultrasound-mediated microbubble destruction improves cardiac function via an angiogenic response. J Mol Cell Cardiol 2006; 40: 799-809.
[27] Ling ZY, Shu SY, Zhong SG, Luo J, Su L, Liu ZZ, Lan XB, Yuan GB, Zheng YY, Ran HT, Wang ZG and Yin YH. Ultrasound targeted microbubble destruction promotes angiogenesis and heart function by inducing myocardial microenvironment change. Ultrasound Med Biol 2013; 39: 2001-2010.
[28] Song J, Cottler PS, Klibanov AL, Kaul S and Price RJ. Microvascular remodeling and accelerated hyperemia blood flow restoration in arterially occluded skeletal muscle exposed to ultrasonic microbubble destruction. Physiol Heart Circ Physiol 2004; 287: H2754-2761.
[29] Tong J, Ding J, Shen X, Chen L, Bian Y, Ma G, Yao Y and Yang F. Mesenchymal stem cell transplantation enhancement in myocardial infarction rat model under ultrasound com-

bined with nitric oxide microbubbles. PLoS One 2013; 8: e80186.
[30] Wollert KC, Drexler H. Clinical application of stem cells for the heart. Circ Res 2005; 96: 151-63.
[31] Kang HJ, Kim HS, Zhang SY, Park KW, Cho HJ, Koo BK, Kim YJ, Soo Lee D, Sohn DW, Han KS, Oh BH, Lee MM and Park YB. Effects of intracoronary infusion of peripheral blood stem -cells mobilised with granulocyte-colony stimulating factor on left ventricular systolic function and restenosis after coronary stenting in myocardial infarction: the MAGIC cell randomised clinical trial. Lancet 2004; 363: 751-756.
[32] Brunner S, Huber BC, Fischer R, Groebner M, Hacker M, David R, Zaruba MM, Vallaster M, Rischpler C, Wilke A, Gerbitz A and Franz WM. G-CSF treatment after myocardial infarction: impact on bone marrow -derived vs cardiac progenitor cells. Exp Hematol 2008; 36: 695-702.
[33] Chiu RC. Adult stem cell therapy for heart failure. Expe Opin Biol Ther 2003; 3: 215-225.
[34] Siminiak T, Czepcczynski R and Grygieska B. Evidence for extravasation of intacoronary administered bone-marrow derived CD34 + stem cells in patients with acute myocardial infarction. Circulation 2004; 110: III-51.
[35] Li JY, Xu Z and Ma G. An experimental study of ultrasound microbubble destruction in enhancing the efficiency of bone marrow stem cell transplantation. Chinese Journal of Practical Medicine 2007; 2: 4-5.
[36] Xu YL, Gao YH, Fang ZQ, Tan KB, Liu Z and Yang X. Diagnostic ultrasound microbubble destruction enhances homing of bone marrow mesenchymal stem cell to rabbit ischemic myocardium. Journal of Ultrasound Medicine 2008; 17: 899-902.
[37] Xu YL, Gao YH, Liu Z, Tan KB, Hua X, Fang ZQ, Wang YL, Wang YJ, Xia HM and Zhuo ZX. Myocardium-targeted transplantation of mesenchymal stem cells by diagnostic ultrasound-mediated microbubbles destruction improves cardiac function in myocardial infarction of New Zealand rabbits. Int J Cardiol 2010; 138: 182-195.
[38] Strauer BE, Brehm M, Zeus T, Köstering M, Hernandez A, Sorg RV, Kögler G and Wernet P. Repair of infarcted myocardium by autologous intracoronary mononuclear bone marrow cell transplantation in humans. Circulation 2002; 106: 1913-1918.
[39] Zhang WZ, Zha DG, Bin JP, Liu J, Wang P, Wu HB, Huang ZH, Zhou ZJ, Li Q and Liu YL. Preliminary clinical application of contrast echocardiography myocardial in evaluation of myocardial viability. Di Yi Jun Yi Da Xue Xue Bao 2001; 21: 940.